

The Eurasia Proceedings of Science, Technology, Engineering and Mathematics (EPSTEM), 2025

Volume 33, Pages 1-19

IConTech 2025: International Conference on Technology

LMI-Based H-Infinity Controller Design for Missile Guidance Control

Oktay Malci

Yıldız Technical University

Meral Bayraktar

Yıldız Technical University,

Hakan Yazici

Yıldız Technical University

Abstract: In this study, a state-space model of a representative missile was developed to analyze its dynamic behavior under various input conditions. Using MATLAB simulations, the system's responses to different control inputs were examined to understand the missile's natural dynamics and response characteristics. Subsequently, an LMI-based H-infinity controller was designed to enhance the stability and performance of the missile guidance system. The controller was developed by formulating an optimization problem within the Linear Matrix Inequalities (LMI) framework, ensuring maximum stability and disturbance attenuation. The control design also incorporated input saturation constraints and reference tracking by augmenting the system with integral action. The designed controller was implemented and tested in MATLAB, and its effectiveness was evaluated based on system stability, disturbance attenuation. The LMI-based design approach allowed the control gains to be optimally determined, considering external disturbances. Simulation results demonstrate that the LMI-based H-infinity controller provides superior stability and improved disturbance attenuation. This study highlights that LMI-based optimization techniques can be effectively applied to missile guidance systems, offering a powerful tool for managing dynamic uncertainties and external disturbances.

Keywords: Missile guidance, Linear matrix inequality, H-Infinity, Optimization, System dynamics

Introduction

Missile guidance and control systems play a critical role in ensuring precision engagement capabilities under dynamic and uncertain operational environments. These systems must cope with aerodynamic nonlinearities, external disturbances and rapid time-varying conditions, all while maintaining stability and accuracy. Over the past few decades, various control strategies have been developed to address these challenges, including classical PID controllers, optimal control techniques, and more recently, methods that ensure reliable performance under uncertain conditions.

Advanced control theory, particularly H_∞ control, has been extensively studied for aerospace applications due to its ability to attenuate the effect of worst-case disturbances and model uncertainties (Etkin, 1972; Etkin & Reid, 1996; Mackenroth, 2004). The H_∞ framework provides mathematical tools for shaping closed-loop performance through the minimization of the transfer function norm between disturbance inputs and performance outputs (Boyd et al., 1994). Linear Matrix Inequality (LMI) formulations have further facilitated the practical implementation of advanced control laws, enabling the inclusion of multiple design constraints within a convex optimization framework (Duan & Yu, 2013).

- This is an Open Access article distributed under the terms of the Creative Commons Attribution-Noncommercial 4.0 Unported License, permitting all non-commercial use, distribution, and reproduction in any medium, provided the original work is properly cited.

- Selection and peer-review under responsibility of the Organizing Committee of the Conference

© 2025 Published by ISRES Publishing: www.isres.org

In the context of missile guidance, various strategies have been explored in the literature, such as Proportional Navigation (PN), augmented PN, and Pure Pursuit guidance (Siouris, 2004; Yanushevsky, 2007). While these strategies provide intuitive and effective target engagement mechanisms, their integration with modern control theory remains an area of active research, (Nielsen, 1960; Zarchan, 2012). Furthermore, simplifying assumptions such as constant speed and small angle approximations are often adopted to linearize the inherently nonlinear missile dynamics, leading to decoupled longitudinal and lateral-directional state-space models suitable for control synthesis (Stevens et al., 2015).

In this study, a state-space missile model is constructed by applying linearization around an equilibrium condition under standard assumptions. The model incorporates aerodynamic forces and moments based on control surface inputs and flight conditions. A Pure Pursuit guidance law is employed to generate reference attitude commands, and H_∞ controller is designed via LMI optimization to ensure closed-loop stability and disturbance rejection. The proposed control approach is validated through MATLAB/Simulink simulations under both nominal and disturbed scenarios, demonstrating the effectiveness and reliability of the controller.

Conceptual Background

Guidance, navigation, and control systems constitute fundamental components of modern missile technologies. In these systems, ensuring accurate guidance towards the target and maintaining stability against external disturbances are of paramount importance. In this study, the missile model is based on the Skid-to-Turn (STT) principle. In STT-type missiles, directional control is achieved by applying lateral and vertical forces without altering the nose orientation of the airframe. This approach allows for a simpler and more efficient control structure.

The missile motion was modeled using six degrees of freedom (6-DOF) equations of motion, defined with respect to the Earth-Fixed Inertial Frame reference system. Force and moment equations were derived, aerodynamic coefficients were calculated using Athena Vortex Lattice (AVL) software, and the system was linearized separately for the longitudinal and lateral-directional planes. Previous studies have shown that linearized missile guidance models can yield highly accurate performance predictions under certain assumptions, making them a valid foundation for control design (Zarchan, 2012).

In this study, the Pure Pursuit guidance method is employed to generate the reference attitude commands for the missile. In the Pure Pursuit approach, the missile continuously points its nose directly toward the target by aligning its velocity vector with the line-of-sight vector to the target. This strategy provides a simple yet effective mechanism for target interception. The generated reference signals for the pitch and yaw angles guide the missile towards the target position during flight.

During the modeling process, several fundamental assumptions were adopted to simplify the system dynamics. First, the missile was treated as a rigid body, ignoring any structural deformation. The curvature of the Earth and Coriolis effects were also neglected, assuming a flat Earth model. Small angle approximations were applied during the linearization stage to facilitate analytical derivations. Finally, the missile was assumed to maintain a constant forward velocity throughout the flight. A basic guidance method was adopted to generate reference orientation angles for the missile, which will be detailed in subsequent sections. This method aligns with the objectives of achieving a simple and effective orientation control structure in this study.

Mathematical Modeling

Axis Systems

In order to accurately model the missile dynamics, it is necessary to define reference frames associated with both the Earth and the missile itself. In this study, two primary reference frames are used: the Earth-Fixed Inertial Frame and the Body-Fixed Frame as shown in Figure 1. The definitions and transformations between these coordinate systems are consistent with those described in modern aerospace dynamics literature 0.

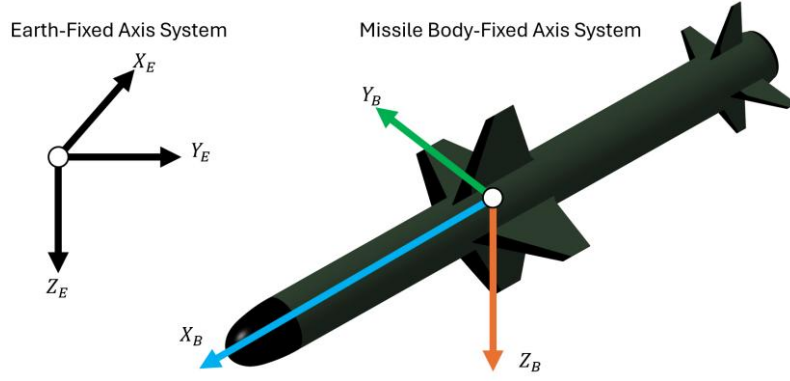


Figure 1. Missile body-fixed axis system and its orientation relative to the earth-fixed inertial frame

Earth-Fixed Inertial Frame

The Earth-Fixed Inertial Frame is a reference coordinate system assumed to be stationary relative to the Earth, and it is used to define the missile's position and velocity. In this frame, the X_E axis points east, the Y_E axis points north, and the Z_E axis is directed downward toward the center of the Earth. Here, the Flat Earth Assumption is adopted, neglecting the curvature and rotation of the Earth. Therefore, the Earth-Fixed Frame is considered inertial.

Body-Fixed Frame

The Body-Fixed Frame is a moving coordinate system attached to the missile. In this frame, the X_B axis points forward along the missile's nose, the Y_B axis points toward the right wing, and the Z_B axis is directed downward. The missile's body dynamics are expressed in terms of forces and moments defined with respect to this coordinate system.

Transformation Matrices

The transformation between the Earth-Fixed Inertial Frame and the Body-Fixed Frame is defined using Euler angles. In this transformation, Yaw (ψ) represents the rotation about the vertical Z_E axis, Pitch (θ) represents the rotation about the lateral Y_B axis, and Roll (ϕ) represents the rotation about the longitudinal X_B axis. Using these angles, the transformation matrix from the Body Frame to the Earth Frame is expressed as:

$$C_{B/E} = \begin{bmatrix} \cos\theta\cos\psi & \cos\theta\sin\psi & -\sin\theta \\ \sin\phi\sin\theta\cos\psi - \cos\phi\sin\psi & \sin\phi\sin\theta\sin\psi + \cos\phi\cos\psi & \sin\phi\cos\theta \\ \cos\phi\sin\theta\cos\psi + \sin\phi\sin\psi & \cos\phi\sin\theta\sin\psi - \sin\phi\cos\psi & \cos\phi\cos\theta \end{bmatrix} \quad (1)$$

where ϕ is the Roll angle, θ is the Pitch angle and ψ is the Yaw angle. This transformation matrix enables the conversion of vectors defined in the Body Frame into the Earth-Fixed Frame.

Force Equations

The forces acting on the missile consist of aerodynamic forces and gravitational forces. Since a constant forward velocity is assumed in this study, thrust force is not included in the model. The aerodynamic force components are defined with respect to the body-fixed frame as follows:

$$F_X = \frac{1}{2} \rho V_T^2 S C_X \quad (2)$$

$$F_Y = \frac{1}{2} \rho V_T^2 S C_Y \quad (3)$$

$$F_Z = \frac{1}{2} \rho V_T^2 S C_Z \quad (4)$$

Here, F_X represents the force acting along the missile's longitudinal axis (forward), F_Y represents the force acting along the lateral axis (side), and F_Z represents the force acting along the vertical axis (downward). ρ denotes the air density, V_T is the total velocity, and S is the reference surface area. The terms C_X , C_Y , and C_Z correspond to the aerodynamic force coefficients along the X, Y, and Z directions, respectively. The gravitational force is defined in the Earth-Fixed Inertial Frame and acts downward. It is transformed into the body-fixed frame using the transformation matrix $C_{B/E}$. The total force vector in the body frame is expressed as:

$$F_B = F_{aero} + C_{B/E}F_{gravity} \quad (5)$$

Moment Equations

The moments acting on the missile originate from aerodynamic effects. In this study, only aerodynamic moments are considered, and engine-generated moments or other external moments are neglected. The aerodynamic moment components are defined with respect to the body-fixed frame as follows:

$$M_X = \frac{1}{2}\rho V_T^2 S l C_L \quad (6)$$

$$M_Y = \frac{1}{2}\rho V_T^2 S l C_M \quad (7)$$

$$M_Z = \frac{1}{2}\rho V_T^2 S l C_N \quad (8)$$

Here, M_X represents the roll moment (rotation about the X-axis), M_Y represents the pitch moment (rotation about the Y-axis), and M_Z represents the yaw moment (rotation about the Z-axis). ρ denotes the air density, V_T is the total velocity, S is the reference surface area, and l is the reference length. The coefficients C_L , C_M , and C_N correspond to the roll, pitch, and yaw moments, respectively. The total aerodynamic moments are expressed with respect to the body-fixed frame and are associated with the changes in angular momentum in the dynamic equations.

Aerodynamic Coefficients and Derivatives

The aerodynamic forces and moments acting on the missile are modeled using specific aerodynamic coefficients. These coefficients are functions of the angle of attack (α), sideslip angle (β), control surface deflections, and angular rates. The aerodynamic force coefficients are defined as:

$$C_X = C_{X_0} + C_{X_\alpha}\alpha + C_{X_q}\frac{ql}{2V} + C_{X_{\delta_e}}\delta_e \quad (9)$$

$$C_Y = C_{Y_\beta}\beta + C_{Y_p}\frac{pl}{2V} + C_{Y_r}\frac{rl}{2V} + C_{Y_{\delta_a}}\delta_a + C_{Y_{\delta_r}}\delta_r \quad (10)$$

$$C_Z = C_{Z_0} + C_{Z_\alpha}\alpha + C_{Z_q}\frac{ql}{2V} + C_{Z_{\delta_e}}\delta_e \quad (11)$$

The aerodynamic moment coefficients are defined as:

$$C_L = C_{L_\beta}\beta + C_{L_p}\frac{pl}{2V} + C_{L_r}\frac{rl}{2V} + C_{L_{\delta_a}}\delta_a + C_{L_{\delta_r}}\delta_r \quad (12)$$

$$C_M = C_{M_0} + C_{M_\alpha}\alpha + C_{M_q}\frac{ql}{2V} + C_{M_{\delta_e}}\delta_e \quad (13)$$

$$C_N = C_{N_\beta}\beta + C_{N_p}\frac{pl}{2V} + C_{N_r}\frac{rl}{2V} + C_{N_{\delta_a}}\delta_a + C_{N_{\delta_r}}\delta_r \quad (14)$$

Here, α represents the angle of attack, β denotes the sideslip angle, p is the roll rate (angular velocity about the X-axis), q is the pitch rate (angular velocity about the Y-axis), and r is the yaw rate (angular velocity about the Z-axis). The terms δ_e , δ_a , and δ_r correspond to the elevator, aileron, and rudder control surface deflections, respectively. Additionally, l denotes the reference length, and V_T is the total velocity. The theoretical framework for aerodynamic coefficient modeling in this study aligns with classical missile aerodynamics formulations presented by Nielsen (1960). The aerodynamic stability and control derivatives used in this study were obtained using the AVL (Athena Vortex Lattice) software. The derivative values were computed based on nine different

combinations of angle of attack (α) and sideslip angle (β) values, each selected as -15° , 0° and 15° . These derivatives were directly integrated into the linearized missile dynamics model.

Table 1 summarizes the aerodynamic derivatives and their physical meanings.

Table 1. Aerodynamic derivatives and their physical meanings	
Symbol	Physical Meaning
$C_{X\alpha}$	X-force coefficient derivative with respect to angle of attack (α)
C_{Xq}	X-force coefficient derivative with respect to pitch rate (q)
$C_{X\delta_e}$	X-force coefficient derivative with respect to elevator deflection (δ_e)
$C_{Y\beta}$	Side force coefficient derivative with respect to sideslip angle (β)
C_{Yp}	Side force coefficient derivative with respect to roll rate (p)
C_{Yr}	Side force coefficient derivative with respect to yaw rate (r)
$C_{Y\delta_a}$	Side force coefficient derivative with respect to aileron deflection (δ_a)
$C_{Y\delta_r}$	Side force coefficient derivative with respect to rudder deflection (δ_r)
$C_{l\beta}$	Roll moment coefficient derivative with respect to sideslip angle (β)
C_{lp}	Roll moment coefficient derivative with respect to roll rate (p)
C_{lr}	Roll moment coefficient derivative with respect to yaw rate (r)
$C_{l\delta_a}$	Roll moment coefficient derivative with respect to aileron deflection (δ_a)
$C_{l\delta_r}$	Roll moment coefficient derivative with respect to rudder deflection (δ_r)
$C_{n\beta}$	Yaw moment coefficient derivative with respect to sideslip angle (β)
C_{np}	Yaw moment coefficient derivative with respect to roll rate (p)
C_{nr}	Yaw moment coefficient derivative with respect to yaw rate (r)
$C_{n\delta_a}$	Yaw moment coefficient derivative with respect to aileron deflection (δ_a)
$C_{n\delta_r}$	Yaw moment coefficient derivative with respect to rudder deflection (δ_r)
$C_{Z\alpha}$	Normal force coefficient derivative with respect to angle of attack (α)
C_{Zq}	Normal force coefficient derivative with respect to pitch rate (q)
$C_{Z\delta_e}$	Normal force coefficient derivative with respect to elevator deflection (δ_e)
$C_{m\alpha}$	Pitch moment coefficient derivative with respect to angle of attack (α)
C_{mq}	Pitch moment coefficient derivative with respect to pitch rate (q)
$C_{m\delta_e}$	Pitch moment coefficient derivative with respect to elevator deflection (δ_e)

Flight Parameters

In the modeling of missile dynamics, flight parameters play a crucial role in defining the system's state variables. In Figure 2, the following flight parameters are illustrated. Forward Velocity (u) is the missile's velocity component along the body-fixed X-axis. It is assumed to be constant throughout the analysis. Also, Angle of Attack (α) is the angle between the body X-axis and the forward velocity vector. It is used under the small angle assumption.

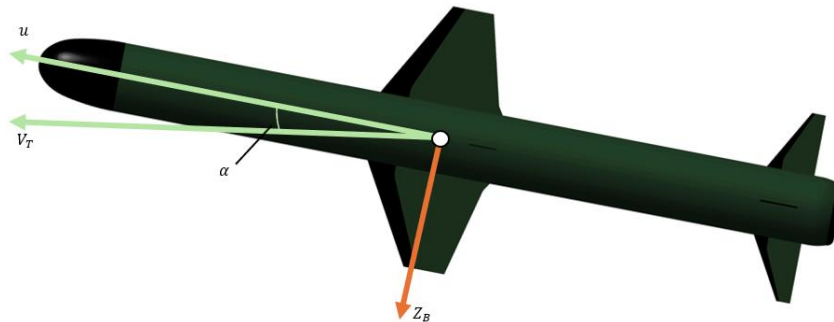


Figure 2. Angle of attack (α) definition

In Figure 3, the Sideslip Angle (β) is shown. It is the angle between the body X-axis and the projection of the velocity vector on the Y-Z plane. It is used under the small angle assumption.

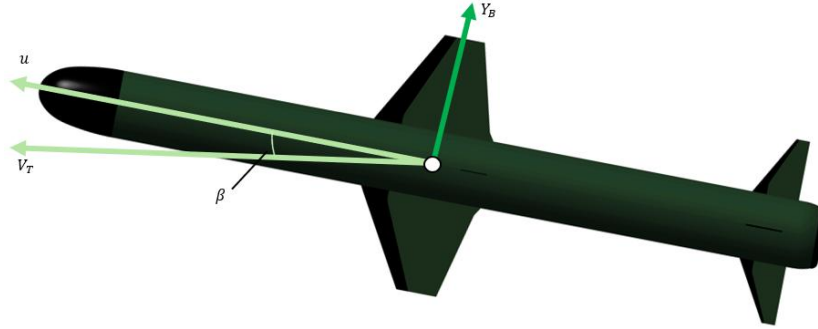


Figure 3. Sideslip angle (β) definition

These parameters are fundamental in the linearization of the missile model and in the formulation of the state-space representation. The use of these parameters and assumptions in missile flight modeling is well established in classical flight dynamics literature (Etkin, 1972).

Translational Kinematic Equations

The translational motion of the missile in the Earth-Fixed Inertial Frame can be represented using the body-fixed velocity components u , v , w and the Euler angles ϕ , θ , ψ . This formulation provides the foundation for describing the missile's motion in three-dimensional space with respect to its center of mass.

$$\dot{X} = u \cos \theta \cos \psi + v(\sin \phi \sin \theta \cos \psi - \cos \phi \sin \psi) + w(\cos \phi \sin \theta \cos \psi + \sin \phi \sin \psi) \quad (15)$$

$$\dot{Y} = u \cos \theta \sin \psi + v(\sin \phi \sin \theta \sin \psi + \cos \phi \cos \psi) + w(\cos \phi \sin \theta \sin \psi - \sin \phi \cos \psi) \quad (16)$$

$$\dot{Z} = -u \sin \theta + v \sin \phi \cos \theta + w \cos \phi \cos \theta \quad (17)$$

These equations describe the instantaneous translational velocity of the missile's center of mass in the Earth-Fixed Inertial Frame and form the basis for modeling the translational dynamics of the missile. Here, u , v and w represent the velocity components along the body-fixed X, Y, and Z axes, respectively. These equations describe the instantaneous translational velocity of the missile's center of mass in the Earth-Fixed Inertial Frame and serve as the basis for modeling the translational dynamics of the missile.

Rotational Kinematic Equations

The orientation changes of the missile are described using Euler angles (ϕ , θ , ψ), and their time derivatives are expressed in terms of the body-fixed angular rates (p , q , r). The rotational kinematic equations for the Euler angles are given as:

$$\dot{\phi} = p + \tan \theta (q \sin \phi + r \cos \phi) \quad (18)$$

$$\dot{\theta} = q \cos \phi - r \sin \phi \quad (19)$$

$$\dot{\psi} = \frac{q \sin \phi + r \cos \phi}{\cos \theta} \quad (20)$$

These equations describe the evolution of the missile's orientation over time based on the angular rates and provide the kinematic model of the rotational motion. This formulation of rotational motion based on Euler angle derivatives is directly aligned with the classical treatment in (Etkin & Reid, 1996).

Linearization

To enable the missile dynamics to be used in control system design, the nonlinear equations of motion are linearized under specific simplifying assumptions. The key assumptions include the small-angle approximation, where angles such as the angle of attack (α), sideslip angle (β), and roll angle (ϕ) are considered small enough to justify the linear relations $\sin \alpha \approx \alpha$, $\cos \alpha \approx 1$, $\sin \beta \approx \beta$, $\sin \psi \approx \psi$, $\sin \phi \approx \phi$, and $\cos \phi \approx 1$. Additionally,

the forward velocity component u is assumed to be constant throughout the flight, leading to the simplification $\dot{u} \approx 0$. Under the mentioned assumptions, the nonlinear equations of motion are linearized around small perturbations from an equilibrium condition. Following the linearization, the system dynamics are decoupled into two independent subsystems: the longitudinal and the lateral-directional planes. The longitudinal plane includes the states w , q , θ , and Z , which represent vertical velocity, pitch rate, pitch angle, and vertical position, respectively. The lateral-directional plane consists of the states v , p , r , ϕ , ψ , and Y , representing lateral velocity, roll rate, yaw rate, roll angle, yaw angle, and lateral position. Separate state-space models are derived for each plane, and the control design is carried out individually based on these linearized subsystems.

State-Space Representation

The linearized missile dynamics are expressed in state-space form separately for the longitudinal and lateral-directional planes. Independent state and input vectors are defined for each plane, and system matrices are constructed accordingly.

Longitudinal Plane State-Space Model

State and input vectors:

$$x_{lon} = [w, q, \theta, Z]^T \quad (21)$$

$$u_{lon} = [\delta_e] \quad (22)$$

State-space equations:

$$\dot{x}_{lon} = A_{lon}x_{lon} + B_{1lon}W_{lon} + B_{2lon}u_{lon} \quad (23)$$

System matrices:

$$A_{lon} = \begin{bmatrix} Z_w & Z_q & -u & 0 \\ M_w & M_q & 0 & 0 \\ 0 & 1 & 0 & 0 \\ 0 & 0 & -u & 0 \end{bmatrix} \quad (24)$$

$$B_{1lon} = [1 \ 1 \ 0 \ 0]^T \quad (25)$$

$$B_{2lon} = [Z_{\delta_e} \ M_{\delta_e} \ 0 \ 0]^T \quad (26)$$

The elements of the system matrices are defined as follows:

$$Z_w = \frac{\rho V_T S_{ref}}{M_{missile}} \cdot C_{Z\alpha} \quad (27)$$

$$Z_q = \frac{\rho S_{ref} l}{2 M_{missile}} \cdot C_{Zq} \quad (28)$$

$$M_w = \frac{\rho V_T S_{ref} l}{I_{yy}} \cdot C_{m\alpha} \quad (29)$$

$$M_q = \frac{\rho S_{ref} l^2}{2 I_{yy}} \cdot C_{mq} \quad (30)$$

$$Z_{\delta_e} = \frac{\rho V_T^2 S_{ref}}{M_{missile}} \cdot C_{Z\delta_e} \quad (31)$$

$$M_{\delta_e} = \frac{\rho V_T^2 S_{ref} l}{I_{yy}} \cdot C_{m\delta_e} \quad (32)$$

Lateral-Directional Plane State-Space Model

State and input vectors:

$$x_{lat} = [v, p, r, \phi, \psi, Y]^T \quad (33)$$

$$u_{lat} = [\delta_a, \delta_r] \quad (34)$$

State-space equations:

$$\dot{x}_{lat} = A_{lat}x_{lat} + B_{1lat}W_{lat} + B_{2lat}u_{lat} \quad (35)$$

System matrices:

$$A_{lat} = \begin{bmatrix} Y_v & Y_p & Y_r & -g \cos(\theta_0) & 0 & 0 \\ L_v & L_p & L_r & 0 & 0 & 0 \\ N_v & N_p & N_r & 0 & 0 & 0 \\ 0 & 1 & 0 & 0 & 0 & 0 \\ 0 & 0 & 1 & 0 & 0 & 0 \\ 1 & 0 & 0 & 0 & 0 & 0 \end{bmatrix} \quad (36)$$

$$B_{1lat} = [1 \ 0 \ 1 \ 0 \ 0 \ 0]^T \quad (37)$$

$$B_{2lat} = \begin{bmatrix} Y_{\delta_a} & L_{\delta_a} & N_{\delta_a} & 0 & 0 & 0 \\ Y_{\delta_r} & L_{\delta_r} & N_{\delta_r} & 0 & 0 & 0 \end{bmatrix}^T \quad (38)$$

The elements of the system matrices are defined as follows:

$$Y_v = \frac{\rho V_T S_{ref}}{M_{missile}} \cdot C_{Y\beta} \quad (39)$$

$$Y_p = \frac{\rho S_{ref} l}{2M_{missile}} \cdot C_{Yp} \quad (40)$$

$$Y_r = \frac{\rho S_{ref} l}{2M_{missile}} \cdot C_{Yr} \quad (41)$$

$$L_v = \frac{\rho V_T S_{ref} l}{I_{xx}} \cdot C_{l\beta} \quad (42)$$

$$L_p = \frac{\rho S_{ref}^2 l}{2I_{xx}} \cdot C_{lp} \quad (43)$$

$$L_r = \frac{\rho S_{ref}^2 l}{2I_{xx}} \cdot C_{lr} \quad (44)$$

$$N_v = \frac{\rho V_T S_{ref} l}{I_{zz}} \cdot C_{n\beta} \quad (45)$$

$$N_p = \frac{\rho S_{ref}^2 l}{2I_{zz}} \cdot C_{np} \quad (46)$$

$$N_r = \frac{\rho S_{ref}^2 l}{2I_{zz}} \cdot C_{nr} \quad (47)$$

$$Y_{\delta_a} = \frac{\rho V_T^2 S_{ref} l}{M_{missile}} \cdot C_{Y\delta_a} \quad (48)$$

$$Y_{\delta_r} = \frac{\rho V_T^2 S_{ref} l}{M_{missile}} \cdot C_{Y\delta_r} \quad (49)$$

$$L_{\delta_a} = \frac{\rho V_T^2 S_{ref} l}{I_{xx}} \cdot C_{l\delta_a} \quad (50)$$

$$L_{\delta_r} = \frac{\rho V_T^2 S_{ref} l}{I_{xx}} \cdot C_{l\delta_r} \quad (51)$$

$$N_{\delta_a} = \frac{\rho V_T^2 S_{ref} l}{I_{zz}} \cdot C_{n\delta_a} \quad (52)$$

$$N_{\delta_r} = \frac{\rho V_T^2 S_{ref} l}{I_{zz}} \cdot C_{n\delta_r} \quad (53)$$

Pure Pursuit Guidance Law

In the Pure Pursuit guidance method, the missile continuously adjusts its flight path to directly aim at the instantaneous position of the target. The missile aligns its velocity vector with the line-of-sight (LOS) vector to the target at every moment. This principle ensures that the missile always attempts to minimize the angular separation between its own heading and the target's location. Although Pure Pursuit is simple to implement and highly intuitive, it may not guarantee interception against highly maneuverable targets, as the missile may tend to follow a curved path that lags behind rapid target movements. Nevertheless, for stationary or low-maneuvering targets, Pure Pursuit provides an effective and computationally efficient guidance strategy, and it is classified under direct (external) guidance methods as illustrated in Figure 4 (Siouris, 2004).

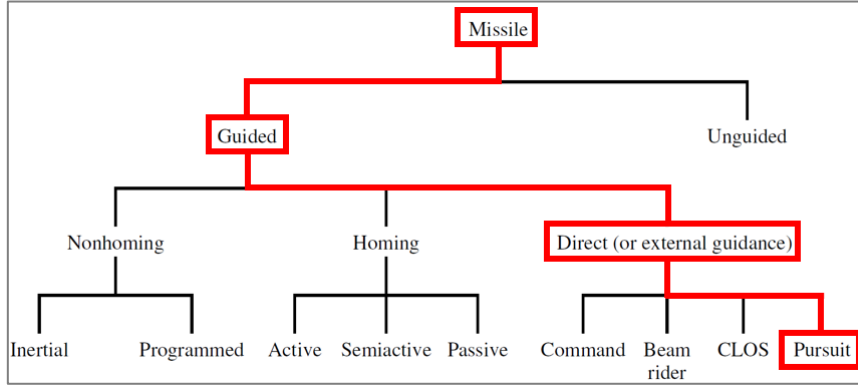


Figure 4. Common missile guidance methods (Adapted from George M. Siouris, Missile Guidance and Control Systems, 2004)

Various studies have examined the integration of classical guidance laws such as Pure Pursuit into modern missile control frameworks. In order to steer the missile toward the target position, reference attitude angles are generated using a Pure Pursuit guidance law. The procedure is as follows:

First, the target direction vector is calculated:

$$V_{Target} = \begin{bmatrix} X_{Target} - x \\ Y_{Target} - y \\ Z_{Target} - z \end{bmatrix} \quad (54)$$

Then, the direction vector is normalized:

$$V_{Dir} = \frac{V_{Target}}{\|V_{Target}\|} \quad (55)$$

The reference yaw angle (ψ_{ref}) is computed as:

$$\psi_{ref} = \arctan2(V_{Dir,y}, V_{Dir,x}) \quad (56)$$

The reference pitch angle (θ_{ref}) is computed as:

$$\theta_{ref} = \arctan2(-V_{Dir,z}, \sqrt{V_{Dir,x}^2 + V_{Dir,y}^2}) \quad (57)$$

The reference roll angle (ϕ_{ref}) is set to zero:

$$\phi_{ref} = 0 \quad (58)$$

Since the missile model adopts a Skid-to-Turn (STT) control architecture where roll dynamics are not actively utilized during the guidance phase. This simple approach allows the missile to dynamically adjust its orientation towards the target throughout the flight, as illustrated in Figure 5.

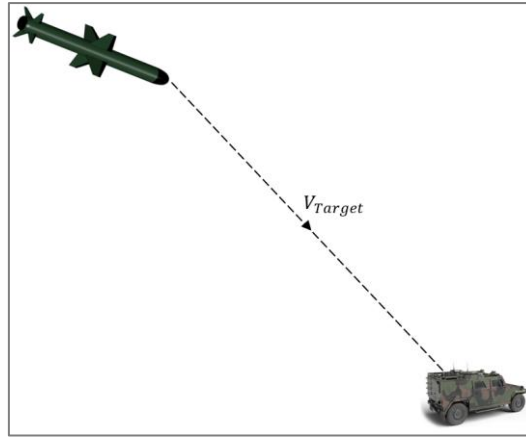


Figure 5. Representation of the target direction vector

Control Design

Control Objectives

The main objectives of the control design for the missile system are summarized in Figure 6. These objectives include ensuring stability in the presence of external disturbances, minimizing their effects through disturbance attenuation, and achieving optimal performance by minimizing the H^∞ norm. Such objectives align closely with the goals of advanced control theory, which aims to maintain performance despite modeling errors and unmeasured perturbations (Mackenroth, 2004).

In this study, the disturbance input is selectively introduced into the angular channels, specifically affecting the pitch (θ) and yaw (ψ) angles, in the form of zero-mean white noise. These perturbations represent realistic environmental effects such as sensor noise or aerodynamic uncertainties. These objectives are addressed through an H^∞ optimization framework formulated using Linear Matrix Inequalities (LMI), which explicitly incorporates stability and disturbance attenuation into the design process.

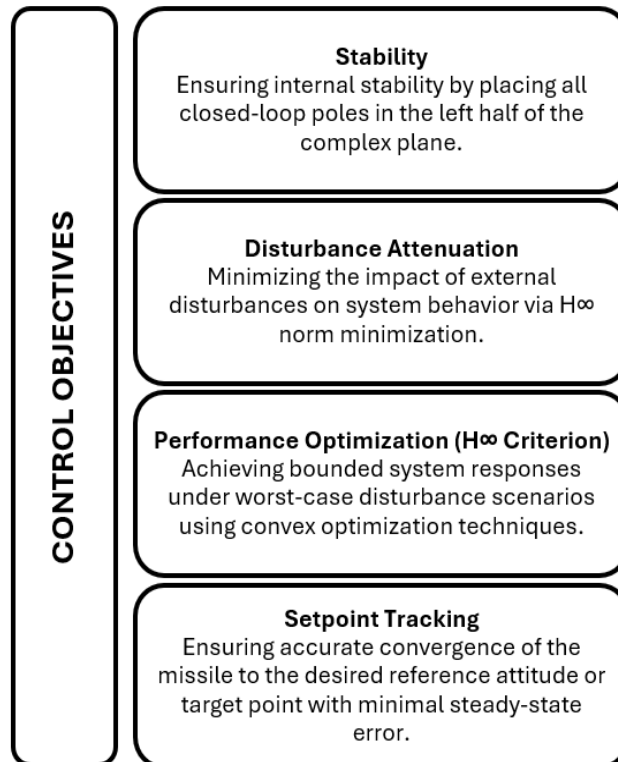


Figure 6. Summary of control objectives considered in the H^∞ -based missile guidance design

State-Feedback H_∞ Controller Design

In order to analyze the closed-loop performance of the missile guidance system under external disturbances, the design equations for a static state-feedback H_∞ controller have been obtained (Boyd et al., 1994). The missile dynamics are represented in the linearized state-space form as:

$$\dot{x}(t) = Ax(t) + B_1w(t) + B_2u(t) + B_{ref}r(t) \quad (59)$$

$$z(t) = C_1x(t) + D_{11}w(t) + D_{12}u(t) \quad (60)$$

In this representation, $x(t) \in R^n$ denotes the state vector of the system, while $w(t) \in R^{m_w}$ represents the exogenous disturbance input acting on the system. The signal $r(t) \in R^{m_r}$ is the reference command, introduced into the system via the input matrix B_{ref} . The term $u(t) \in R^{m_u}$ corresponds to the control input applied to the system. The performance output $z(t) \in R^p$ is defined as the performance variable, which is minimized in the H_∞ sense to ensure stability performance under disturbances. The matrices C_1 , D_{11} , and D_{12} define how the performance output depends on the state, disturbance, and control input, respectively.

To incorporate reference tracking into the H_∞ control framework, the state-space model is augmented with an integral action on the tracking error. This is achieved by extending the system matrices to include the integral of the error between the reference signal $r(t)$ and the corresponding state variable. The extended state vector, input matrices, and output matrices are defined as follows:

$$\begin{bmatrix} \dot{x}(t) \\ e(t) \end{bmatrix} = \begin{bmatrix} A & 0 \\ -C_t & 0 \end{bmatrix} \begin{bmatrix} x(t) \\ \int e(t) \end{bmatrix} + \begin{bmatrix} B_1 \\ 0 \end{bmatrix} w(t) + \begin{bmatrix} B_2 \\ 0 \end{bmatrix} u(t) + \begin{bmatrix} 0 \\ I \end{bmatrix} r(t) \quad (61)$$

Suppose that the control input is linear function of the state, i.e.,

$$u(t) = Kx(t) \quad (62)$$

where $K \in \mathcal{R}^{m_u \times n}$ is the state feedback gain. The closed-loop system is given by

$$\dot{x}(t) = (A + B_2K)x(t) + B_1w(t) \quad (63)$$

$$z(t) = (C_1 + D_{12}K)x(t) + D_{11}w(t) \quad (64)$$

The state-feedback H_∞ controller design is carried out separately for the longitudinal and lateral-directional motion planes. For each case, the control gain K is obtained by solving a convex optimization problem subject to Linear Matrix Inequality (LMI) constraints derived from the bounded real lemma. In addition to performance criteria, input saturation bounds are imposed to ensure that the control signals remain within physically meaningful limits. The optimal nominal H_∞ state-feedback controller can be obtained by searching minimum allowable γ , which satisfies the following LMI for $X = X^T > 0$ and any matrix L .

$$\begin{bmatrix} AX + XA^T + B_2L + L^TB_2^T & B_1 & XC_1^T + L^TD_{12}^T \\ B_1^T & -\gamma I & D_{11}^T \\ C_1X + D_{12}L & D_{11} & -\gamma I \end{bmatrix} < 0 \quad (65)$$

$$\begin{bmatrix} X & L^T \\ L & U_{max}^2 I \end{bmatrix} > 0 \quad (66)$$

$$\begin{bmatrix} Y & I \\ I & X \end{bmatrix} > 0 \quad (67)$$

where U_{max} denotes the maximum allowable deflection for the corresponding control surfaces. If there exists a feasible solution to the optimization problem (65), (66) and (67), the optimal H_∞ state-feedback controller can be constructed as $K = LX^{-1}$.

The objective is to ensure that the control input does not exceed a predefined magnitude bound for all admissible system trajectories (Parlakı & Kucukdemiral, 2010). Assuming that the control input is subject to a magnitude constraint expressed as $\|u\|_2 \leq u_{max}$, where u is the control input and u_{max} denotes the saturation threshold. Based on the definition of the Euclidean norm:

$$\|u\|_2 \leq u_{max} \Leftrightarrow \sqrt{u^T u} \leq u_{max} \Leftrightarrow u^T u \leq u_{max}^2 \quad (68)$$

Since $u(t) = Kx(t)$ and $L = KX$, we can express the condition as:

$$\frac{x^T(t)X^{-1}L^T L X^{-1}x(t)}{u_{max}^2} \leq 1 \quad (69)$$

If we define the ellipsoidal set \mathcal{E}_p as:

$$\mathcal{E}_p = \{x | x^T(t)P x(t) \leq 1\} \quad (70)$$

then inequality (69) becomes equivalent to:

$$x(t) \in \mathcal{E}_{\frac{X^{-1}L^T L X^{-1}}{u_{max}^2}} \quad (71)$$

To ensure that all admissible state trajectories remain within the control bounds, we require:

$$\mathcal{E}_{X^{-1}} \subseteq \mathcal{E}_{\frac{X^{-1}L^T L X^{-1}}{u_{max}^2}} \quad (72)$$

This is equivalent to the matrix inequality:

$$X^{-1} \geq \frac{X^{-1}L^T L X^{-1}}{u_{max}^2} \quad (73)$$

To simplify inequality (73) a congruence transformation is performed. Both sides are pre- and post-multiplied X resulting in:

$$X \geq \frac{L^T L}{u_{max}^2} \quad (74)$$

which, by Schur complement (Boyd et al.,2004), is equivalently expressed as:

$$\begin{bmatrix} X & L^T \\ L & u_{max}^2 I \end{bmatrix} \geq 0 \quad (75)$$

It is worth noting that so far, the enlargement of the ellipsoid has not been addressed. Geometrically, the volume of the ellipsoid $\mathcal{E}_{X^{-1}}$ is proportional to $\sqrt{\det(X^{-1})}$. Given that:

$$\sqrt{\det(X^{-1})} \leq \left(\frac{\text{trace}(X^{-1})}{n} \right)^n \quad (76)$$

it is reasonable to minimize X^{-1} . However, since X^{-1} is not directly a decision variable, we define an auxiliary variable $Y = Y^{-T} \geq X^{-1}$. Then, minimizing $\text{trace}(Y)$ provides an ellipsoid enlargement objective. Using Schur complement again, the constraint $Y \geq X^{-1}$ is rewritten as:

$$Y - I X^{-1} I > 0 \Leftrightarrow \begin{bmatrix} Y & I \\ I & X \end{bmatrix} \geq 0 \quad (77)$$

In this study, the control signal limit was chosen as $u_{max} = 30^\circ$, reflecting the maximum allowable deflection of the control surfaces. This value was used directly in the actuator saturation LMI condition during controller synthesis. The LMI optimization problem was implemented and solved in MATLAB using the YALMIP toolbox, with MOSEK employed as the underlying convex optimization solver. This computational setup provided reliable and efficient handling of matrix inequality constraints under numerical precision.

Simulation Study

In this section, numerical simulations are conducted to evaluate the performance of the designed H_∞ state-feedback controllers under external disturbances and reference tracking requirements. The missile model is

analyzed separately in the longitudinal and lateral-directional motion planes, using the extended state-space formulation described previously. The closed-loop response is examined with respect to stability, disturbance attenuation, and control effort limitations.

Longitudinal Motion Plane

The extended state-space matrices for the longitudinal motion plane, augmented for reference tracking, are given as follows:

$$A_{lon} = \begin{bmatrix} Z_w & Z_q & -u & 0 & 0 \\ M_w & M_q & 0 & 0 & 0 \\ 0 & 1 & 0 & 0 & 0 \\ 0 & 0 & -u & 0 & 0 \\ 0 & 0 & -1 & 0 & 0 \end{bmatrix} \quad (78)$$

$$B_{1lon} = [0 \ 1 \ 0 \ 0 \ 0]^T \quad (79)$$

$$B_{2lon} = [Z_{\delta_e} \ M_{\delta_e} \ 0 \ 0 \ 0]^T \quad (80)$$

$$B_{reflon} = [0 \ 0 \ 0 \ 0 \ 1]^T \quad (81)$$

$$C_{1lon} = \begin{bmatrix} 0 & 0 & -1 & 0 & 0 \\ 0 & 0 & 0 & 0 & 1 \end{bmatrix} \begin{matrix} \text{(Selection of } -\theta) \\ \text{(Selection of } \int e_\theta(t)) \end{matrix} \quad (82)$$

$$D_{11lon} = [0 \ 0]^T \quad (83)$$

$$D_{12lon} = [0 \ 0]^T \quad (84)$$

Lateral-Directional Motion Plane

The extended system matrices for the lateral-directional motion plane are constructed similarly. The augmented state-space model used for controller synthesis is represented as follows:

$$A_{lat} = \begin{bmatrix} Y_v & Y_p & Y_r & -g \cos(\theta_0) & 0 & 0 & 0 & 0 \\ L_v & L_p & L_r & 0 & 0 & 0 & 0 & 0 \\ N_v & N_p & N_r & 0 & 0 & 0 & 0 & 0 \\ 0 & 1 & 0 & 0 & 0 & 0 & 0 & 0 \\ 0 & 0 & 1 & 0 & 0 & 0 & 0 & 0 \\ 1 & 0 & 0 & 0 & u & 0 & 0 & 0 \\ 0 & 0 & 0 & -1 & 0 & 0 & 0 & 0 \\ 0 & 0 & 0 & 0 & -1 & 0 & 0 & 0 \\ 0 & 0 & 0 & 0 & 0 & -1 & 0 & 0 \end{bmatrix} \quad (85)$$

$$B_{1lat} = [0 \ 0 \ 1 \ 0 \ 0 \ 0 \ 0 \ 0]^T \quad (86)$$

$$B_{2lat} = \begin{bmatrix} Y_{\delta_a} & L_{\delta_a} & N_{\delta_a} & 0 & 0 & 0 & 0 & 0 \\ Y_{\delta_r} & L_{\delta_r} & N_{\delta_r} & 0 & 0 & 0 & 0 & 0 \end{bmatrix}^T \quad (87)$$

$$B_{reflat} = \begin{bmatrix} 0 & 0 & 0 & 0 & 0 & 0 & 1 & 0 \\ 0 & 0 & 0 & 0 & 0 & 0 & 0 & 1 \end{bmatrix}^T \quad (88)$$

$$C_{1lat} = \begin{bmatrix} 0 & 0 & 0 & -1 & 0 & 0 & 0 & 0 \\ 0 & 0 & 0 & 0 & -1 & 0 & 0 & 0 \\ 0 & 0 & 0 & 0 & 0 & 0 & 1 & 0 \\ 0 & 0 & 0 & 0 & 0 & 0 & 0 & 1 \end{bmatrix} \begin{matrix} \text{(Selection of } -\phi) \\ \text{(Selection of } -\psi) \\ \text{(Selection of } \int e_\phi(t)) \\ \text{(Selection of } \int e_\psi(t)) \end{matrix} \quad (89)$$

$$D_{11lat} = [0 \ 0 \ 0 \ 0]^T \quad (90)$$

$$D_{12lat} = \begin{bmatrix} 0 & 0 & 0 & 0 \\ 0 & 0 & 0 & 0 \end{bmatrix}^T \quad (91)$$

Controller Synthesis Results

In this section, the definitions of the state trajectory $\dot{x}(t)$ and performance output $z(t)$, which are used in the H_∞ controller synthesis, are provided explicitly for both the longitudinal and lateral-directional subsystems. Below, the resulting expressions for $\dot{x}_{lon}(t)$, $z_{lon}(t)$, $\dot{x}_{lat}(t)$ and $z_{lat}(t)$ are provided accordingly.

$$\dot{x}_{lon} = A_{lon}x_{lon}(t) + B_{1lon}w_{lon}(t) + B_{2lon}u_{lon}(t) + B_{reflon}\theta_{ref} \quad (92)$$

$$z_{lon}(t) = C_{1lon}x_{lon}(t) + D_{11lon}w_{lon}(t) + D_{12lon}u_{lon}(t) \quad (93)$$

$$\dot{x}_{lat} = A_{lat}x_{lat} + B_{1lat}w_{lat} + B_{2lat}u_{lat} + B_{reflat}[\phi_{ref}, \psi_{ref}] \quad (94)$$

$$z_{lat}(t) = C_{1lat}x_{lat}(t) + D_{11lat}w_{lat}(t) + D_{12lat}u_{lat}(t) \quad (95)$$

To obtain the optimal state feedback gains K_{lon} and K_{lat} the optimization problem is formulated as minimizing the γ performance bound subject to the LMI conditions given in (65), (66) and (67). These constraints ensure the H_∞ performance requirement. The optimal control gain for suppressing the disturbances affecting the system with the state feedback control law is achieved by solving

$$\begin{aligned} & \min \gamma \\ & \text{Constraints: (65), (66) and (67)} \end{aligned}$$

optimization problem. This solution is solved for 9 cases each for the Longitudinal Plane and Lateral-Directional Plane. The cases are given in Table 2. In the simulation, control gains corresponding to different flight conditions were determined from a predefined set of nine operating scenarios, created by varying angle of attack (α) and sideslip angle (β) values. The gain matrices were stored in a structured look-up table, enabling the controller to dynamically select appropriate feedback gains according to the current flight condition.

Table 2 Flight condition cases used for controller synthesis

Case	Angle of Attack (α) [Degree]	Sideslip Angle (β) [Degree]	Mach	Altitude [m]
1	-15	-15		
2	-15	0		
3	-15	15		
4	0	-15		
5	0	0	0.6	1000
6	0	15		
7	15	-15		
8	15	0		
9	15	15		

The solution to this optimization problem yields different γ performance levels for each defined flight condition. Table 3 summarizes the minimum closed-loop γ values obtained for each case, separately for the longitudinal and lateral-directional motion planes.

Table 3 Closed-loop γ values for longitudinal and lateral-directional planes

Case	Longitudinal Closed-Loop γ	Lateral-Directional Closed-Loop γ
1	0.0175	14.7850
2	0.0160	12.9523
3	0.0180	64.9524
4	0.0159	271.3944
5	0.0146	226.3793
6	0.0160	233.3257
7	0.0177	37.1123
8	0.0161	22.3868
9	0.0177	37.8336

The optimal state feedback gain matrices K , computed for each defined flight condition, are presented in Table 4. Each gain matrix is computed individually using the LMI-based synthesis approach and is associated with one of the predefined operating conditions. It is important to note that the open-loop system exhibits instability under all evaluated flight conditions. As a result, analyzing the open-loop H_∞ performance level (γ) is not meaningful, and such values are therefore omitted from the comparison. Instead, the effectiveness of the proposed state-feedback controller is assessed through the minimum closed-loop γ values obtained from the LMI-based optimization. As shown in Table 3, the closed-loop γ values for the longitudinal motion plane are consistently low across all nine flight cases, indicating reliable disturbance attenuation and strong stability performance along the longitudinal axis. In the lateral-directional plane, the closed-loop γ values vary more significantly depending on the sideslip angle and angle of attack, yet remain within an acceptable range. Additionally, closed-loop stability analysis has been performed by evaluating the eigenvalues of the system matrices under each flight condition. In all cases, the eigenvalues are located in the left-half complex plane, confirming that the designed controller ensures asymptotic stability of the closed-loop system in both motion planes.

Table 4. State feedback gain matrices (K) for each case

Case	Longitudinal	Lateral-Directional
1	$K_{lon1} = [-0.0020 \quad 0.2637 \quad 1.5379 \quad 0.0 \quad -1.6587]$	$K_{lat1} = \begin{bmatrix} -5.2450 & 17.4657 & 0.9132 & 30.0508 & 0.5136 & 0.0 & -0.1534 & -0.1251 \\ 1.8144 & -6.1221 & -1.8803 & -10.4746 & -1.0268 & 0.0 & 0.1428 & 0.2510 \end{bmatrix}$
2	$K_{lon2} = [-0.0018 \quad 0.2567 \quad 1.5589 \quad 0.0 \quad -1.7109]$	$K_{lat2} = \begin{bmatrix} -4.748 & 14.5610 & 0.5657 & 26.1161 & 0.3464 & 0.0 & -0.1559 & -0.0941 \\ 1.6784 & -5.2236 & -1.7203 & -9.3085 & 0.9521 & 0.0 & 0.1464 & 0.2383 \end{bmatrix}$
3	$K_{lon3} = [-0.0018 \quad 0.2613 \quad 1.5072 \quad 0.0 \quad -1.6327]$	$K_{lat3} = \begin{bmatrix} -2.4412 & 8.1303 & 0.4167 & 13.9871 & 0.1268 & 0.0 & -0.0789 & -0.0178 \\ -0.3078 & 0.9868 & -1.1389 & 1.7587 & -0.4278 & 0.0 & -0.0272 & 0.0726 \end{bmatrix}$
4	$K_{lon4} = [-0.0022 \quad 0.2574 \quad 1.5693 \quad 0.0 \quad -1.7131]$	$K_{lat4} = \begin{bmatrix} -0.0038 & 4.4404 & -0.0390 & 0.9337 & 0.0137 & 0.0 & -0.0461 & 0.0002 \\ -0.0253 & 0.0590 & -0.8086 & 0.3342 & -0.2440 & 0.0 & 0.0029 & 0.0335 \end{bmatrix}$
5	$K_{lon5} = [-0.0020 \quad 0.2504 \quad 1.5897 \quad 0.0 \quad -1.7702]$	$K_{lat5} = \begin{bmatrix} -0.0041 & 3.4551 & -0.0452 & 0.8394 & 0.0169 & 0.0 & -0.0468 & -0.0008 \\ -0.0262 & 0.1214 & -0.8002 & 0.3461 & -0.2547 & 0.0 & 0.0027 & 0.0374 \end{bmatrix}$
6	$K_{lon6} = [-0.0020 \quad 0.2567 \quad 1.5589 \quad 0.0 \quad -1.7359]$	$K_{lat6} = \begin{bmatrix} -0.0056 & 3.2778 & -0.0610 & 0.8632 & 0.0174 & 0.0 & -0.0459 & -0.0011 \\ -0.0293 & 0.1987 & -0.8455 & 0.4027 & -0.2654 & 0.0 & 0.0030 & 0.0397 \end{bmatrix}$
7	$K_{lon7} = [-0.0023 \quad 0.2631 \quad 1.5283 \quad 0.0 \quad -1.7275]$	$K_{lat7} = \begin{bmatrix} 2.1981 & 4.9679 & -0.9032 & -2.3137 & -0.3299 & 0.0 & -0.1816 & 0.0536 \\ 0.0097 & -2.5254 & -1.0155 & -5.4980 & -0.3944 & 0.0 & 0.0908 & 0.0720 \end{bmatrix}$
8	$K_{lon8} = [-0.0023 \quad 0.2567 \quad 1.5583 \quad 0.0 \quad -1.7617]$	$K_{lat8} = \begin{bmatrix} 2.1049 & 5.1919 & -1.0891 & -1.4278 & -0.4386 & 0.0 & -0.1682 & 0.0812 \\ 0.0976 & -1.8277 & -1.1078 & -4.5925 & -0.4878 & 0.0 & 0.1122 & 0.1012 \end{bmatrix}$
9	$K_{lon9} = [-0.0022 \quad 0.2631 \quad 1.5272 \quad 0.0 \quad -1.7286]$	$K_{lat9} = \begin{bmatrix} 1.9502 & 5.0097 & -0.8772 & -0.7729 & -0.3273 & 0.0 & -0.1894 & 0.0539 \\ 0.0346 & -2.2077 & -1.0556 & -4.9718 & -0.4129 & 0.0 & 0.0833 & 0.0754 \end{bmatrix}$

Results

To evaluate the system's resilience against external disturbances, zero-mean white noise signals were introduced into the pitch (θ) and yaw (ψ) channels. Figure 7 displays the disturbance signals applied over time. These inputs exhibit continuous, stochastic variations, simulating real-world aerodynamic uncertainties. The disturbance amplitudes remain within physically reasonable bounds and serve as a meaningful benchmark to test the control structure.

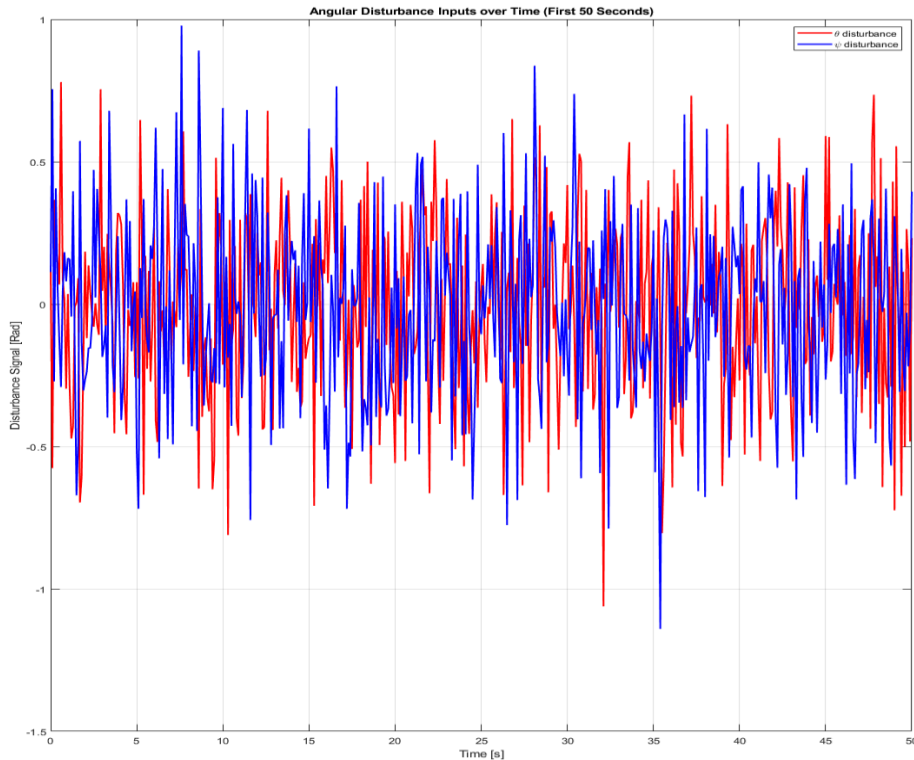


Figure 7. Disturbance signals applied to pitch (θ) and yaw (ψ) channels in the form of zero-mean white noise

The effectiveness of the proposed H_∞ controllers is evaluated through time-domain simulations involving reaching the desired position and external disturbances. In the primary scenario, the missile is commanded to reach a spatial reference position at coordinates $X, Y, Z = 40000, 40000, 40000$ meters as seen in Figure 8. In the absence of external disturbances, the terminal position error is approximately 27 meters. Remarkably, when zero-mean white noise is introduced into the pitch and yaw channels, the deviation reduces slightly to 26 meters. This counterintuitive improvement is attributed to the dynamic characteristics of the controller, which actively attenuates disturbance effects and guides the missile along a smooth trajectory.

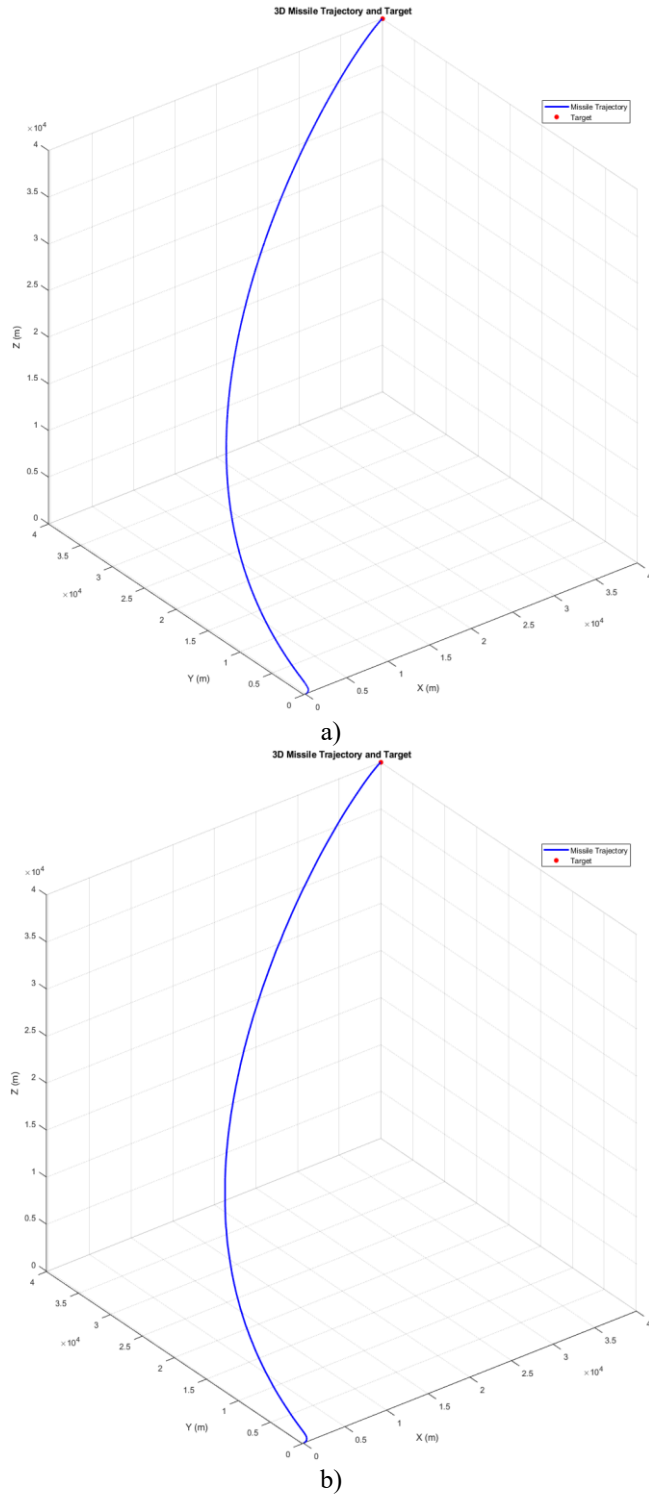
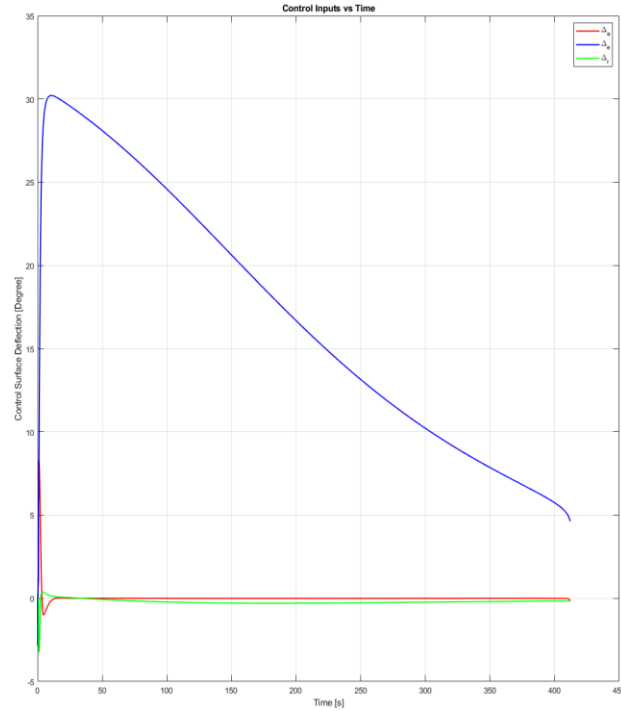
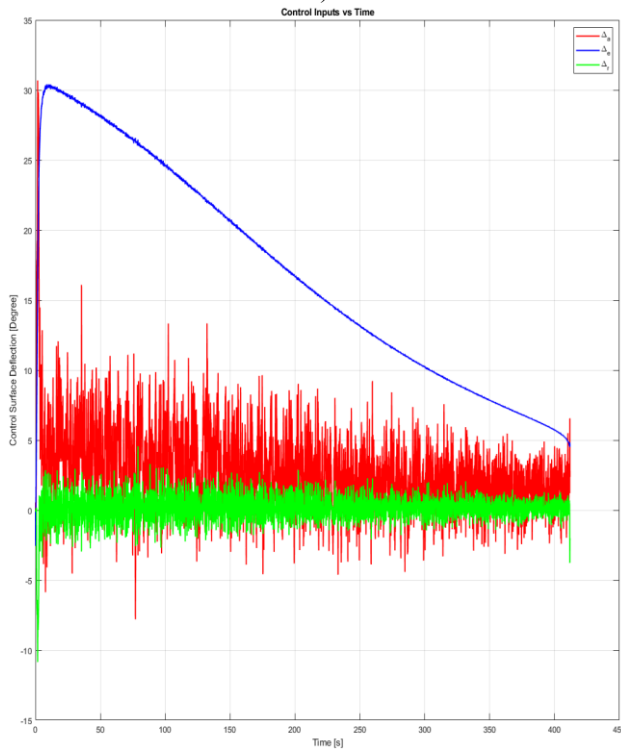


Figure 8. Missile trajectory under a) nominal conditions without external disturbances b) disturbance conditions (white noise applied to θ and ψ)

In addition, the control surface deflections generated by the designed controller are examined to ensure that actuator constraints are respected. Figure 9 presents the control inputs (aileron, elevator, and rudder deflections) over time for both nominal and disturbance cases. In both scenarios, the control signals remain within the acceptable range, not exceeding approximately 30 degrees, which corresponds to the predefined actuator limits imposed during the LMI-based synthesis. The deflection signals exhibit smooth and bounded behavior, confirming that the controller operates effectively without driving the actuators into saturation. Moreover, the similarity of the control profiles between the nominal and disturbance cases highlights the robustness of the control structure against external perturbations.



a)



b)

Figure 9. Control surface deflections for a) nominal conditions without external disturbances b) disturbance conditions (white noise applied to θ and ψ)

Discussion

The simulation results confirm that the proposed H_∞ controller provides reliable performance in missile trajectory tracking and disturbance rejection across a variety of flight conditions. Notably, the closed-loop system maintains stability and control effectiveness even when subject to continuous white noise disturbances applied to critical angular states. The final position error with respect to the spatial reference remains within tight bounds, and actuator deflections stay below physical saturation levels, which validates the practicality of the designed control law under operational constraints.

Conclusion

In this study, an H_∞ state-feedback controller was developed for missile guidance applications using an LMI-based synthesis framework. The missile dynamics were modeled separately for longitudinal and lateral-directional planes in a linearized state-space form, with aerodynamic stability and control derivatives derived via AVL simulations. The control design incorporated input saturation constraints and reference tracking by augmenting the system with integral action. Time-domain simulations were conducted across multiple flight conditions, including the presence of white noise disturbances applied to pitch and yaw angles.

Results demonstrate that the proposed controller enables the missile to reach a spatial reference target with high precision, maintaining final position errors under approximately 30 degrees and keeping control inputs within actuator limits. The system remained stable under all tested conditions, confirming the effectiveness and practical viability of the approach. This LMI-based H_∞ control methodology provides a promising solution for advanced missile guidance systems requiring consistent performance under varying operational scenarios and external disturbances.

Recommendations

Based on the findings of this study, several directions are suggested to further improve missile guidance control strategies. One promising avenue is the development of hybrid H_2/H_∞ controllers, which could offer a balanced trade-off between disturbance attenuation and control effort, thereby enhancing overall system efficiency. Additionally, extending the controller design to nonlinear missile models would provide a more realistic assessment of flight dynamics, especially under extreme operating conditions. The incorporation of adaptive or gain-scheduled control techniques may also increase the controller's flexibility in handling model uncertainties and changing flight regimes. Finally, validating the proposed method through hardware-in-the-loop simulations or physical test platforms is essential to ensure its practical feasibility and real-time implementation capability. These extensions would collectively support the development of more robust, intelligent, and adaptable missile guidance systems.

Scientific Ethics Declaration

* The authors declare that the scientific ethical and legal responsibility of this article published in EPSTEM Journal belongs to the authors.

Conflict of Interest

* The authors declare that they have no conflicts of interest.

Funding

The authors declare that no specific funding was received from any agency in the public, commercial, or non-profit sectors for this research.

Acknowledgements or Notes

* This article was presented as an oral presentation at the International Conference on Technology (www.icontechno.net) held in Trabzon/Türkiye on May 01-04, 2025.

References

- Boyd, S., El Ghaoui, L., Feron, E., & Balakrishnan, V. (1994). *Linear matrix inequalities in system and control theory*. SIAM.
- Duan, G. R., & Yu, H.-H. (2013). *LMIs in control systems: Analysis, design and applications*. CRC Press.
- Etkin, B. (1972). *Dynamics of atmospheric flight*. John Wiley & Sons.
- Etkin, B., & Reid, L. D. (1996). *Dynamics of flight: Stability and control* (3rd ed.). Wiley.
- Mackenroth, U. (2004). *Robust control systems: Theory and case studies*. Springer.
- Nielsen, J. N. (1960). *Missile aerodynamics*. McGraw-Hill.
- Parlakçı, M. N. A., & Kucukdemiral, I. B. (2010). \mathcal{L}_2 -gain control of time-delay systems with actuator saturation. *International Conference on System Science and Engineering (ICSSE)*, 263–268.
- Siouris, G. M. (2004). *Missile guidance and control systems*. Springer.
- Stevens, B. L., Lewis, F. L., & Johnson, E. N. (2015). *Aircraft control and simulation: Dynamics, Controls Design, and Autonomous Systems* (3rd ed.). Wiley.
- Yanushevsky, R. (2007). *Modern missile guidance*. CRC Press.
- Zarchan, P. (2012). *Tactical and strategic missile guidance* (6th ed.). American Institute of Aeronautics and Astronautics (AIAA).

Author Information

Oktay Malci

Yıldız Technical University, Department of Mechanical Engineering, Istanbul, Türkiye
Contact e-mail: oktaymalci@gmail.com

Meral Bayraktar

Assoc. Prof. Dr.
Yıldız Technical University, Department of Mechanical Engineering, Istanbul, Türkiye

Hakan Yazici

Assoc. Prof. Dr.
Yıldız Technical University, Department of Mechanical Engineering, Istanbul, Türkiye

To cite this article:

Malci, O., Bayraktar, M., & Yazici, H. (2025). LMI-based H-infinity controller design for missile guidance control. *The Eurasia Proceedings of Science, Technology, Engineering and Mathematics (EPSTEM)*, 33, 1-19.